Available online at www.sciencedirect.com
ScienceDirect
Journal of Molecular Catalysis A: Chemical 262 (2007) 59–66
JOURNAL OF MOLECULAR CATALYSIS A: CHEMICAL
www.elsevier.com/locate/molcata

Electron capture and transport by heteropolyanions: Multi-functional electrolytes for biomass-based fuel cells

Yurii V. Geletii [a], Andrei Gueletii [a], Ira A. Weinstock [b,*]

[a] *Department of Chemistry, Emory University, Atlanta, GA 30322, USA*
[b] *Department of Chemistry, City College of New York, New York, NY 10031, USA*

Available online 1 September 2006

Abstract

Keggin heteropolyanions (POMs) are evaluated for use as an alternative to H_2 in the storage and transfer of electrons from alcohols (ROH) to O_2 in biomass-based electrochemical energy-conversion devices. Pt(0) (present as 10 wt.% Pt on C) is used to catalyze the oxidation of alcohols under mild conditions by α-$H_3PMo_{12}O_{40}$ (H_3**1**) and $H_5PV_2Mo_{10}O_{40}$ (H_5**2**). During these reactions, the POMs efficiently "capture" electron equivalents as they are rapidly reduced by intermediates generated during the Pt(0)-catalyzed oxidation of alcohols. Potentiometric data indicate that this results in the two-electron reduction of **1**, and in substantial reduction of **2**. Kinetic data show that the rate of POM reduction is limited by the rate of ROH activation at Pt. Upon exposure to O_2, Pt(0) catalyses rapid oxidation of the reduced solutions of both **1** and **2** to their (nearly) fully oxidized forms. Possible effects of the POMs on the activity of the Pt catalyst were assessed by measuring rates of Pt(0)-catalyzed O_2-oxidations of EtOH. Here, as in the anaerobic reduction of POMs, activation of EtOH on Pt(0) is rate limiting. Having demonstrated this, Keggin heteropolyanions were added, and their effects on overall rates quantified. In all cases, inhibition was observed, and the effect was more pronounced for Keggin anions with more positive reduction potentials. While the reactions involved are complex, these observations suggest that under certain conditions POMs may inhibit the rate-limiting activation of EtOH by Pt(0).

Keywords: Alcohol oxidation; Dioxygen; Keggin heteropolyanion; Polyoxometalates; Platinum

1. Introduction

1.1. The hydrogen economy and PEM fuel cells

Hydrogen (H_2) has been identified as a promising new "currency" in the portfolio of options available for meeting society's energy needs. One highly publicized use is in the internal combustion engines of "clean" H_2-fueled vehicles [1]. Meanwhile, automobile manufacturers acknowledge [2] that direct combustion is likely to be supplanted by more versatile methods for deriving electrical power from H_2. One option is to use H_2 and O_2 in the anodic and cathodic compartments, respectively, of polyelectrolyte- ("proton-exchange-") membrane (PEM) fuel cells. Commercially viable (inexpensive and efficient) PEM fuel cells – still in development – could be used in transportation, and to provide power for portable devices, such as cell-phones and laptop computers, or even, for entire homes. However, even as the development of PEM-cell technology proceeds, the U.S. still lacks the extensive "hydrogen production, storage and delivery" [3] infrastructure needed for societal use of H_2. This is a widely acknowledged obstacle to the development of a hydrogen economy [3].

1.2. Integrated PEM fuel cells

One attractive solution is to develop multi-functional PEM fuel-cell systems that include integrated "on-demand" H_2 production [4]. In this scenario, petrochemicals, natural gas, or alcohols (e.g. methanol or ethanol), for which extensive production, storage and delivery infrastructure is already in place, would be supplied to the end user, and there "reformed" to give H_2 and CO_2 (an inevitable by-product) in integrated PEM fuel cells [5,6]. A further attractive option is that the alcohols used be derived from renewable-biomass resources, such as agricultural residues (byproducts of agricultural processes), or energy-dedicated crops [5–7]. Use of renewable resources would not only decrease U.S. dependence on foreign oil, but would decrease the impact of power production on global warming:

* Corresponding author.
E-mail address: iraw@bgu.ac.il (I.A. Weinstock).

1381-1169/$ – see front matter © 2006 Elsevier B.V. All rights reserved.
doi:10.1016/j.molcata.2006.08.075

Unlike petrochemicals, which, provided they remain beneath the earth's surface, do not enter the biosphere, carbon from biomass is simply returned to the global carbon cycle as this renewable fuel is converted to its biosynthetic precursors, H_2O and CO_2.

1.3. Advanced biomass-based fuel cells

The use of H_2 in integrated PEM fuel cells faces a number of challenges. One obstacle is that production of H_2 typically results in the co-formation of carbon monoxide (CO), which binds to, and "poisons" the Pt used to catalyze reactions of H_2 in PEM cells [5]. In addition, it would be advantageous (cost and energy efficient) if fuel cells were designed to use not only simple hydrocarbons and alcohols, but, also, more complex agrichemical products, such as glucose, and mixtures of sugars and/or water-soluble polysaccharides [7]. In light of these limitations, it is useful to consider the functional role of H_2 in integrated fuel cells.

1.4. H_2 as electron carrier

In PEM fuel cells, oxidation of H_2 occurs in one compartment, and the electrons removed from H_2 pass through an external circuit before reaching the cathode, where O_2 is reduced to H_2O (the H^+ ions needed to form water diffuse through the proton-exchange membrane, PEM). The electrochemical potential driving this process, and that produces power, is determined by the Gibbs free energy of the reaction between H_2 and O_2. On the other hand, the overall reaction between hydrocarbons or carbohydrates, themselves, and O_2, is very energetically favorable. Thus, in the context of the overall reactions of hydrocarbons or carbohydrates with O_2 in integrated cells, H_2 serves simply as a "carrier" of electron equivalents initially present in the petrochemical- or biomass-derived fuel. The reforming step (conversion of fuel to H_2 and CO_2) is not needed to derive power, but rather, to provide H_2 for reaction with O_2 in the PEM cell. Recognizing this, it is reasonable to question whether electron carriers other than H_2 might be more suitable for the development of versatile, biomass-based fuel cells.

1.5. Heteropolyanions as redox-active electrolytes in biomass-based fuel cells

We here evaluate the use of Keggin heteropolyanions (POMs) as an alternative to H_2 in the storage and transfer of electrons from alcohols to O_2 in biomass-based electrochemical energy-conversion devices. Despite decades of extensive efforts to develop less expensive alternatives, Pt(0) or Pt(0)-containing materials remains the most effective electrocatalysts for use in PEM fuel cells [8,9]. Pt(0) efficiently catalyzes anodic reactions (H_2 and alcohol oxidation) and the reduction of O_2 at the cathode [8,9]. In addition, in POM-based photooxidations of organic molecules, the transfer of electrons to and from organic substrates and H^+/H_2 is catalyzed by Pt(0) [10,11]. In the present study, 10 wt.% Pt(0) on C (Pt/C) is used in combination with a series of POMs to obtain quantitative data concerning key questions pertinent to the possible use of POMs as electron carriers in biomass-based fuel cells. Future work based on these findings could entail the use of late-transition-metal-containing POMs that act, not only as electron carriers, but – replacing the Pt/C used here – as catalysts for their own reduction (by biomass) and/or for the cathodic reduction of O_2 [12].

We first show that Pt(0) catalyzes the reduction of heteropolyanions by alcohols (ROH) under mild conditions. During these reactions, the POMs efficiently "capture" electron equivalents by rapid oxidation of intermediates generated during Pt(0)-catalyzed oxidation of the alcohols. These data show how POMs might function as electron reservoirs in the presence of an alcohol-oxidation catalyst that is separate and distinct from the anodic-electrode itself. In this scenario, electron equivalents in the reduced POMs are carried to the anode, and electrical power is derived from completion of the electrochemical reaction (combustion of ROH) by reduction of O_2 at the cathode.

It is also possible to envision the use of POM electron carriers at the cathode. Here, POMs would receive electrons from the cathode, and transfer these to O_2 in a separate step, distant from the cathodic electrode itself. The challenge here is that, in many cases, thermodynamically favorable electron transfer from reduced Keggin anions to O_2 is slow. We now report that one such typically slow reaction, electron transfer from $\mathbf{1}_{1e}$ (the 1e-reduced form of α-$PMo_{12}O_{40}^{3-}$, **1**) to O_2, is accelerated dramatically by the addition of Pt/C.

Finally, the aerobic Pt(0)-catalyzed oxidation of EtOH in the presence of several Keggin heteropolyanions was used as an indirect probe of possible effects of **1** or **2** ($PV_2Mo_{10}O_{40}^{5-}$) on the activity of the Pt catalyst used in the work described above. In addition to **1** and **2**, the effects of three heteropolytungstates $X^{n+}W_{12}O_{40}^{(n-8)-}$, $X^{n+} = P^{5+}$, Si^{4+} or Al^{3+}, were investigated. While the reactions involved – and attendant mechanistic considerations – are complex, all five heteropolyanions decrease rates of O_2-uptake. Kinetic data show that this inhibition is due to an effect of the POMs on a single rate-limiting process common to both the oxidation of ROH by O_2, and to the anaerobic oxidation of ROH by **1** or **2**: the rate of ROH activation by Pt.

2. Experimental

2.1. Materials

The Keggin heteropolyanions, α-$H_3PW_{12}O_{40}$ and α-$H_3PMo_{12}O_{40}$ (H_5**1**) were purchased from Sigma–Aldrich Inc. and from ACROS, while α-$Na_4SiW_{12}O_{40}$, α-$Na_5AlW_{12}O_{40}$ and $H_5PV_2Mo_{10}O_{40}$ (H_5**2**) were prepared using published methods [13] (in aqueous solution, **2** is the dominant anion in an equilibrated mixture of compounds that includes relatively small concentrations of $PV_1Mo_{11}O_{40}^{4-}$ and $PV_3Mo_9O_{40}^{6-}$, along with positional isomers of the di- and tri-vanadium clusters [14]). Platinum catalyst, 10 wt.% Pt on activated carbon (Pt/C) was purchased from Sigma–Aldrich Inc. Water for the preparation of solutions was obtained from a Barnstead Nanopure® water-purification system, and all other chemicals and salts were of the highest purity available from commercial sources.

2.2. Instrumentation

UV–vis spectra were acquired using a Hewlett-Packard 8452A spectrophotomer equipped with a diode-array detector, a magnetic stirrer and a HP 89090A temperature controller. Electrochemical measurements (cyclic voltammetry and controlled potential coulometry) were performed using a BAS CV-50W electrochemical analyzer equipped with a glassy-carbon working electrode, a Pt-wire auxiliary electrode, and a Ag/AgCl (3 M NaCl) BAS reference electrode. The BAS reference electrode was calibrated as described in [15]. Changes in reduction potentials of solutions of α-$PMo_{12}O_{40}^{3-}$ (**1**) and $PV_2Mo_{10}O_{40}^{5-}$ (**2**) were determined using a Pt-redox electrode (SympHony combination redox electrode, VWR Scientific Products). Dioxygen consumption was determined from a pressure decrease using an Artisan™ digital manometer. Analysis of hydrogen in the reaction headspace was performed using a HP5890A model gas chromatograph equipped with thermo-conductivity detector with a detection level of 0.01 μmol of H_2. High resolution scanning electron microscopy (HRSEM) images were obtained on a DS-130 FESEM instrument operated at 25 kV.

2.3. Reaction procedures and conditions

In stoichiometric reductions of the heteropolyanions, desired amounts of alcohols, acid, salts, and POMs were mixed with water and placed in a beaker. Solutions were continuously purged with Ar (15–20 mL/min). The redox electrode was immersed in the solution. The reaction was then started after temperature equilibration by addition of the solid catalyst.

A similar procedure was used to monitor O_2 consumption. Here, ethanol (EtOH) was used as a model substrate. A Pt(0) catalyst was placed in a reaction vessel that had been purged with O_2, and a solution containing both a POM salt and EtOH was added. The reaction vessel was then sealed with a rubber septum, connected to a manometer, and immersed in a water bath. The reaction mixture was mixed continuously using a magnetic stirrer set at 350 rpm. After the first 3–5 min (needed to seal the reaction vessel and for temperature equilibration), the pressure in the reaction vessel decreased linearly with time as dioxygen was consumed. Rates of dioxygen consumption (i.e. rates of overall reaction of alcohol with dioxygen) were measured at low conversions of EtOH and O_2, less than 10 and 15%, respectively. After each catalytic run all glassware items were thoroughly cleaned in an ultrasonic bath.

2.4. Reaction rates

2.4.1. Anaerobic reactions

Rates for reactions carried out in the absence of O_2 were determined by quantifying the rate of reduction of α-$PMo_{12}O_{40}^{3-}$ (**1**) and $PV_2Mo_{10}O_{40}^{5-}$ (**2**). Rates of reduction were studied under Ar by using a redox electrode to monitor changes in reduction potentials of the POM solutions. To calibrate the electrode, the heteropolymolybdates were quantitatively reduced by bulk electrolysis, during which, the electrochemical potential of the solution was monitored. Potential readings from the redox electrode were plotted as a function of the concentrations of reduced anions formed. Desired concentrations of $PMo_{12}O_{40}^{4-}$ ($\mathbf{1}_{1e}$; the 1e-reduced anion) were obtained by varying the numbers of electrons transferred per cluster anion: $[PMo_{12}O_{40}^{4-}] = Q/FV$, where Q is the total charge (in Coulombs) of the electrons passed, F the Faraday constant and V is the solution volume. The data obtained obeyed the Nernst equation, $E = E_0 - RT/nF([PMo_{12}O_{40}^{3-}]/[PMo_{12}O_{40}^{4-}])$, with a slope 63 ± 3 mV (the theoretical value of RT/nF for $n = 1$ is 59 mV) and $E_0 = 444 \pm 6$ mV. The experimental error in determination of [$\mathbf{1}_{1e}$] was ca. 5%. The same procedure was used to calibrate the electrode with respect to $[PMo_{12}O_{40}^{5-}]$ (the 2e-reduced anion, $\mathbf{1}_{2e}$; the total charge, Q, was equivalent to reduction by two electrons). However, experimental errors in this case were much higher, up to 25%. The reduced forms of **1** could be present as equilibrated mixtures that include small concentrations of β-structural isomers. Because of this, no isomer designations are used as prefixes to the formulas: $PMo_{12}O_{40}^{4-}$ ($\mathbf{1}_{1e}$) or $PMo_{12}O_{40}^{5-}$ ($\mathbf{1}_{2e}$).

2.4.2. Aerobic reactions

Steady-state rates of EtOH oxidation by O_2 were determined by decreases in O_2 pressure in sealed reaction vessels. The solution volumes were 15 or 30 mL, with total overhead volumes, respectively, of 30 and 39 mL. To minimize the effect of decreases in O_2 pressure on solution-O_2 concentrations, total pressure drops never exceeded 120 mm Hg under pure oxygen (760 mm Hg) or 35 mm Hg under air (partial pressure of O_2 = 160 mm Hg).

2.5. Products of EtOH oxidation

Acetaldehyde (a product of ethanol oxidation) was quantified by its color reaction with 3-methyl-2-benzothiazolone hydrazone [16]. This was carried out after aerobic oxidation by Pt(0) in the absence of Keggin anions (because the POMs interfered with this color reaction, analysis of products formed in the presence of the POMs could not be reliably determined). Before reaction with 3-methyl-2-benzothiazolone hydrazone, the Pt(0) catalyst was removed by filtration through Whatman disposable-syringe filters (250 nm, PSU).

3. Results and discussion

3.1. Characterization of Pt/C catalyst

The Pt(0) particles present in the 10 wt.% Pt on activated carbon (Pt/C; from a commercial source) were analyzed by high-resolution scanning electron microscopy (HRSEM). The data show that Pt(0)-particle sizes span a wide range of values, from ca. 6 nm to 1 μm in diameter. They consist of single nanoparticles (4–20 nm, Fig. 1, panel A), clusters of nanoparticles (50–300 nm, panels A and B), and large particles (0.3–1 μm, panel C).

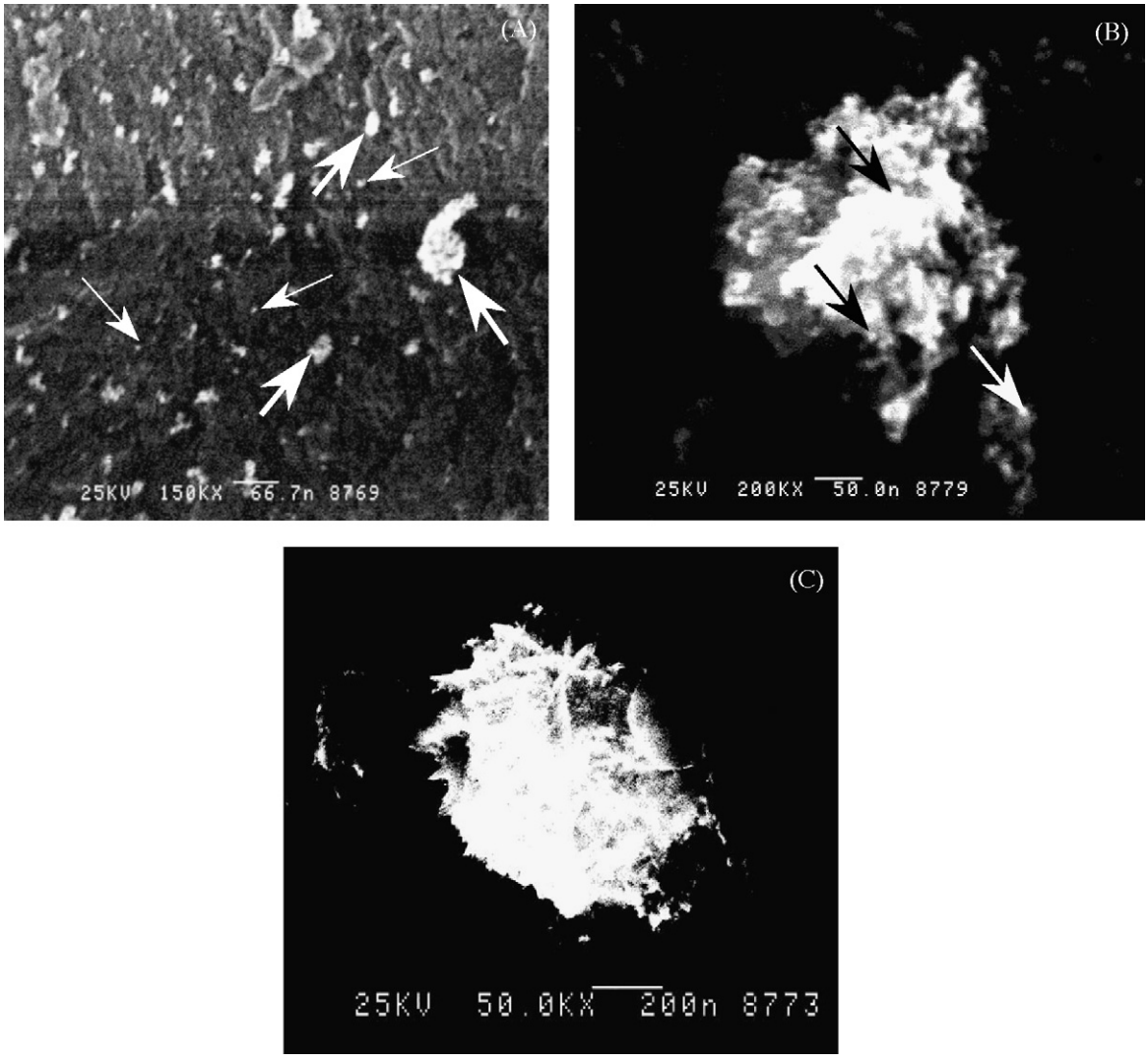

Fig. 1. High resolution scanning electron microscopy (HRSEM) images of the Pt/C catalyst (10 wt.% Pt on activated carbon). Single Pt(0) nanoparticles on carbon, and within clusters of nanoparticles are shown by arrows in panels A and B. Clusters of nanoparticles are shown on panel A (bold arrows) and on panel B. A large Pt-particle is shown on panel C.

3.2. Reductions of Keggin anions during Pt/C-catalyzed anaerobic oxidations of alcohols

Pt/C was used to catalyze the reductions of α-$PMo_{12}O_{40}^{3-}$ (**1**; fully oxidized) to $PMo_{12}O_{40}^{4-}$ ($\mathbf{1}_{1e}$; one-electron reduced) or $PMo_{12}O_{40}^{5-}$ ($\mathbf{1}_{2e}$; two-electron reduced) by alcohols in water at 25 °C. The reductions of **1** caused the chemical potential of the solution to become more negative (data for reduction by EtOH are shown in Fig. 2). These decreases in solution potential were used to monitor the rate, as well as the extent, of reductions of **1** (in reactions involving the formation of reduced POMs, UV–vis spectroscopy is routinely used for this. In the present case, however, obstruction by suspended Pt/C particles made spectrophotometric methods unreliable). During reaction, the electrochemical potential of the solution reached a plateau at ca. 250 mV, which corresponded to > 95% reduction of **1** to $\mathbf{1}_{2e}$ (reduction of each cluster by between 1.9 and 2 electrons). For comparison, the solid circles in Fig. 2 indicate the potential of a pure (alcohol-free) solution of $\mathbf{1}_{2e}$ (effectively 100% of this anion, in $HClO_4$, prepared by constant-potential electrolysis). Electrochemical potentials were also used to monitor the re-oxidation of reduced forms of **1** and **2** upon addition of O_2 in the absence and presence of EtOH (the results, shown at the right in Fig. 2, are discussed below in Section 3.4).

The data on the left side of Fig. 2 show that **1** is an effective oxidant of reactive intermediates of alcohol oxidation present in solution and/or adsorbed onto the Pt/C surface. An extensive chemistry, involving related reactions, is well known for $H_5PV_2Mo_{10}O_{40}$ (**2**; a fully oxidized equilibrated mixture of anions, as described in Section 2) [14,17, and references therein]. Therefore, data obtained using solutions of **2** are included for comparison in Fig. 2.

Rates of Pt/C-catalyzed reductions of **1** by a series of alcohols, polyols, and low-molecular-weight organic compounds, plus H_2, were quantified by decreases in solution potentials. The data were analogous to those shown at the left in Fig. 2. Kinetic curves describing $\mathbf{1}_{1e}$ accumulation were obtained from decrease in the electrochemical potential of the solutions during

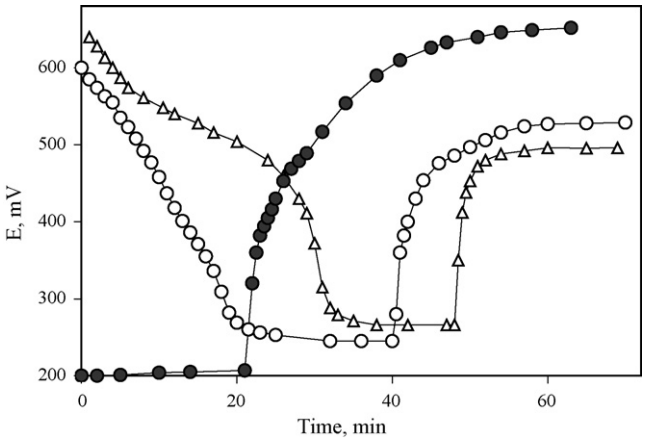

Fig. 2. Solution potentials of α-$PMo_{12}O_{40}^{3-}$ (**1**; open circles, ◯) and $PV_2Mo_{10}O_{40}^{5-}$ (**2**; triangles, △) in 0.1 M $HClO_4$ at 25 °C, during anaerobic Pt/C (1.45 mg/mL) catalyzed reduction by EtOH (0.82 M; left side of figure). The rapid increases in potential (middle and right in the figure) coincide with the addition of pure O_2 by gentle bubbling. Data shown as solid circles (●) indicate the potential of solutions of $\mathbf{1}_{2e}$ (prepared by bulk electrolysis in the absence of EtOH) in 0.1 M $HClO_4$ at 25 °C, first under pure O_2 (left side of the figure), and then, upon addition of Pt/C (1.45 mg/mL) at $t = 20$ min.

the early part of the reaction (from 530 to 390 mV in Fig. 2). The formation of $\mathbf{1}_{1e}$ proceeds with an induction period, which is concentration dependent. For example, the induction period becomes longer with decrease in alcohol concentrations and is longer with less reactive alcohols (e.g. ca. 30 min for glycerol, but 2–3 min for EtOH). After the induction period, the rate of $\mathbf{1}_{1e}$ accumulation remains constant over the remaining initial phase of the reaction. Reported reaction rates refer to slopes of these linear phases (after the induction period).

Rate data for Pt/C-catalyzed reductions of **1** by a number of substrates is provided in Fig. 3.

In the presence of Pt/C, carbon monoxide (CO, 1 atm) [18] and hydrogen (H_2, 1 atm) both reduced **1**. In the absence of Pt, neither reaction is observed at room temperature. After completion of reaction the electrochemical potentials of the solutions in all cases (except when reduced by H_2) were the same, ca.

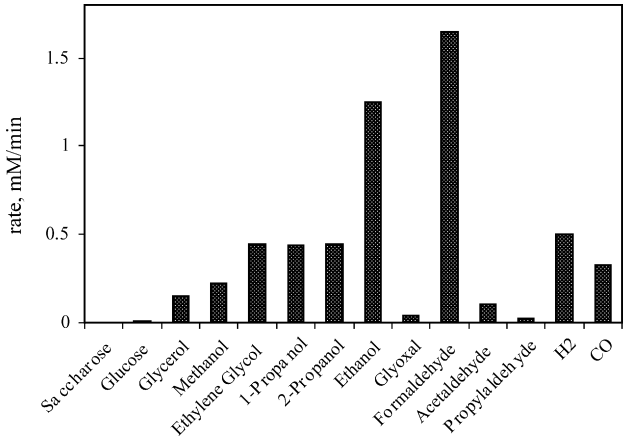

Fig. 3. Initial rates (after variable-time induction periods; see text) for Pt/C (1.2 mg/mL) catalyzed reductions of α-$PMo_{12}O_{40}^{3-}$ (**1**) in 0.1 M $HClO_4$ at 25 °C. The organic compounds listed were each present at 5 wt.%, and pure H_2 and CO gases were bubbled through the solutions at ambient pressure.

250 mV, which corresponds to nearly complete two-electron reduction of α-$PMo_{12}O_{40}^{3-}$ (**1**) to $PMo_{12}O_{40}^{5-}$ ($\mathbf{1}_{2e}$). When H_2 is used, however, the final potential reached after extended reaction times is considerably more negative (−110 mV). These potentials are more positive than the thermodynamic potential required to reduce proton (1 M HCl) to H_2 (1 atm) is 0 mV versus NHE, or −197 mV versus our Ag/AgCl reference electrode. The large difference in achievable solution potentials is consistent with the unfavorable thermodynamics typically associated conversions of alcohols to aldehydes and H_2 in water at ambient temperature [6 and references therein]. In one case (26 μmol **1**, 10 wt.% EtOH, 2.3 mg/mL Pt/C, 0.1 M $HClO_4$, reaction time 24 h), this was confirmed directly: no H_2 was detected in the headspace of the reaction vessel.

*3.3. Effects of pH, reactant concentrations, and the quantity of Pt/C, on the anaerobic reduction of **1***

Reaction with EtOH proceeds rather quickly, which did not allow for collection of accurate data over the range of potentially useful concentrations (0–30 wt.%). Therefore, glycerol was used as a model alcohol to assess the dependence of reaction rate (reduction of **1**) on mechanistically meaningful variables. The rate of reduction of **1** increased linearly with glycerol concentration (0–30 wt.%), and with the quantity of Pt/C (up to 1.8 mg/mL), but was independent of [**1**] (at 2 and 5.3 mM) and $HClO_4$ (0.1–0.33 M).

Control experiments, with no Pt/C present, indicated that **1** does not oxidize glycerol directly. Rather, **1** is reduced by intermediates – in solution, on the metal surface, or possibly present in the carbon support – generated by reactions between glycerol and Pt(0). Notably, independence of the rate on [**1**] indicates that, in anaerobic electron transfer from glycerol to **1**, the rate-of-reduction of **1** is limited by the rate at which the alcohol reacts with Pt(0).

3.4. Pt-catalyzed electron transfer from reduced Keggin anions to O_2

The data on the right side of Fig. 2 show that both $\mathbf{1}_{2e}$ and reduced solutions of **2** are rapidly oxidized by O_2 in the presence of Pt/C. This is true in the absence, as well as in the presence, of EtOH. Both reduced-POM solutions are reoxidized significantly more rapidly than they are reduced, and at similar rates.

It is well known that reduced forms of **2** are rapidly, and fully, oxidized by O_2 at low pH values. The vanadium-free anion, **1**, was evaluated here in more detail. First, solutions of pure $\mathbf{1}_{1e}$ and $\mathbf{1}_{2e}$ (no Pt/C or EtOH present) were prepared by bulk electrolysis under conditions otherwise identical to those used in reactions involving Pt/C and EtOH. Rates of reoxidation by O_2 were monitored both by decrease in absorbance at 700 nm, and by increase in the electrochemical potential of the solution. In the absence of Pt/C, $\mathbf{1}_{1e}$ is kinetically stable under air, while oxidation of $\mathbf{1}_{2e}$ to $\mathbf{1}_{1e}$ is slow. Addition of $Cu(ClO_4)_2$ considerably increases the rate of aerobic oxidation of $\mathbf{1}_{2e}$ to $\mathbf{1}_{1e}$. Even in the presence of Cu ions, however, $\mathbf{1}_{1e}$ is not readily oxidized by O_2 to **1** (i.e. no noticeable changes are observed in the reduction

potentials of these solutions after several hours under 1 atm of O_2).

The solid circles in Fig. 2 show that, under O_2 alone (no EtOH), $\mathbf{1}_{2e}$ is reoxidized very slowly, but is rapidly oxidized to **1** (>99% to its fully oxidized form) upon addition of Pt/C. Additional data in the upper-right portion of Fig. 2 show that, in the presence of Pt/C (and EtOH), O_2-oxidation of $\mathbf{1}_{2e}$ to **1** proceeds quickly, and nearly to completion. Under these steady-state conditions, both molybdophosphate solutions remain slightly reduced (ca. 5% of the anions are reduced by one electron).

These data show that reduced forms of **1** and **2** are rapidly oxidized by O_2 in the presence of Pt(0) [related chemistry is reported in Refs. 10,11]. This demonstrates that it might be possible to use late-transition-metal-containing POMs as soluble electrocatalysts, or for the modification of electrode surfaces, to facilitate more rapid cathodic reduction of O_2.

3.5. Effect of heteropolyanions on the Pt/C-catalyzed aerobic oxidation of EtOH

Additional control experiments were carried out to assess possible effects of **1** and **2**, and of Keggin heteropolytungstates, α-$X^{n+}W_{12}O_{40}^{(8-n)-}$ ($X^{n+} = Al^{3+}$, Si^{4+} and P^{3+}), on the Pt(0)-catalyzed electron-transfer from EtOH to POMs shown in Fig. 2. Their reduction potentials are substantially more negative (55, −145 and −330 mV for $X^{n+} = Al^{3+}$, Si^{4+}, P^{3+}, respectively [15]) than the lowest potentials achieved with alcohols, ca. 250 mV. Therefore, unlike **1** and **2**, the heteropoly*tungstates*, α-$X^{n+}W_{12}O_{40}^{(8-n)-}$, are *not* reduced by EtOH in the presence of Pt/C under Ar. They are included here, however, to more broadly assess the effects of Keggin anions on the activity of the Pt/C catalyst.

For this, Pt/C was used to catalyze the oxidation of EtOH by O_2, and the effects of the heteropolyanions on rates of O_2 consumption were quantified. Given the complexity of both the aerobic and anaerobic reactions, use of the aerobic process to obtain information that might provide insight into reactions occurring in the absence of O_2 *minimally* requires that both processes (aerobic and anaerobic) proceed via a common rate-limiting step. Therefore, these studies were only undertaken after kinetic data (below), clearly identified activation of EtOH on Pt as the rate-limiting step in both reactions: the anaerobic oxidation of EtOH by **1** or **2**, as well as the aerobic oxidation of EtOH by O_2.

First, the Pt/C-catalyzed oxidation of EtOH by O_2 was studied in detail. Reaction rates were measured by quantifying the rate of consumption of O_2. For solutions containing 0.82 M EtOH, and 1.2 mg/mL Pt/C, and saturated with pure O_2 (at 1 atm; ca. 1 mM O_2), the reaction is independent of [$HClO_4$] (from 1 to 300 mM) and [$NaClO_4$] (at concentrations as large as 290 mM, in the presence of 10 mM $HClO_4$). At 0.82 M EtOH, and 0.1 M $HClO_4$, the rate increases linearly with the load of Pt/C catalyst (from 0 to 3.0 mg/mL). At constant Pt/C loading (1.45 mg/mL) and 0.1 M [$HClO_4$], the reaction rate reaches a plateau as [EtOH] is increased (Fig. 4). The data in Fig. 4 also show that under air (an approximately five-fold decrease in the concentration of O_2 in solution), this plateau is reached at smaller EtOH concentrations. In addition, replacement of O_2 by air results in a three-fold decrease in rate at 1.3 M EtOH, but has no effect on the rate 0.16 M EtOH. Acetaldehyde was found to be the dominant product. For example, during the oxidation of 0.82 M EtOH (0.1 M $HClO_4$, 1.45 mg/mL Pt/C), the concentration of acetaldehyde was 7.6 ± 0.5 mM after 25 min, and 12 ± 0.6 mM after 40 min. Associated consumptions of O_2 were 5.0 ± 0.3 mM after 25 min, and 7.7 ± 0.4 after 40 min. If acetaldehyde were the only product, its theoretical yield per O_2 consumed would be 2.0. The experimental ratios are somewhat smaller (approximately 1.5), which is likely due to further oxidation to acetic acid (15%, along with an 85% yield of acetaldehyde). These data are similar to results obtained in Pt-catalyzed electrochemical oxidations of EtOH, in which acetaldehyde is the main product when [EtOH] > 0.15 M [19].

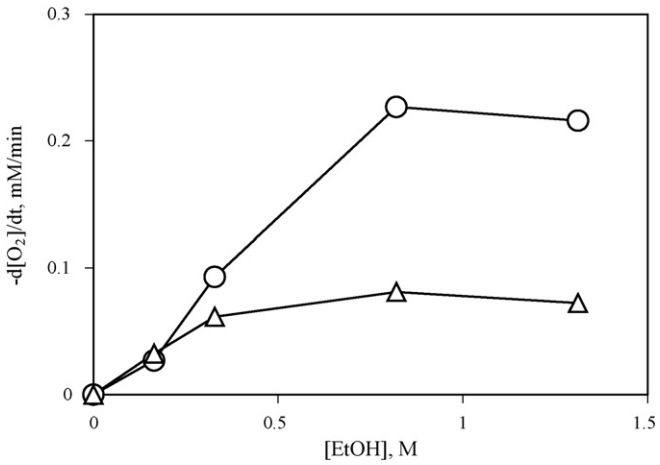

Fig. 4. Rate of dioxygen consumption in EtOH oxidation by pure O_2 (◯) or by air (△) catalyzed by 1.45 mg/mL Pt/C in 0.1 M $HClO_4$ at 25 °C.

Together, the above data demonstrate that at relatively small (<0.82 M) concentrations of EtOH, at a constant loading of Pt, and under pure O_2, the overall rate is limited by reactions of EtOH with the Pt/C catalyst. Having demonstrated this, similar conditions were used to evaluate the effect of Keggin heteropolyanions on the Pt/C-catalyzed O_2-oxidation of EtOH. As is true in the presence of O_2, alcohol activation by Pt/C is also the rate-limiting step in the anaerobic reactions described earlier (left side of Fig. 2, above). Therefore, the effects of POMs on reaction rates in the presence of O_2 was used as an indirect indication as to whether the POMs might effect the activity of Pt/C towards alcohols in the anaerobic reactions in Fig. 2.

Initial rates of aerobic oxidations of EtOH were determined by decrease in O_2 pressure. The results are shown in Fig. 5. In the absence of Keggin anions, the initial rate of EtOH oxidation, indicated by O_2 consumption, was 0.24 mM O_2 min^{-1} (see value on the ordinate for [POM] = 0). In all cases, additions of Keggin heteropoly-tungstates or -molybdates resulted in decreases in rates of uptake of O_2. No correlation was observed between inhibition and anion charge. However, inhibition was less pronounced for anions that possess more negative reduction potentials (cf. α-$AlW_{12}O_{40}^{5-}$), and was more pronounced for anions whose reduction potentials are more positive (cf. **1**, **2**,

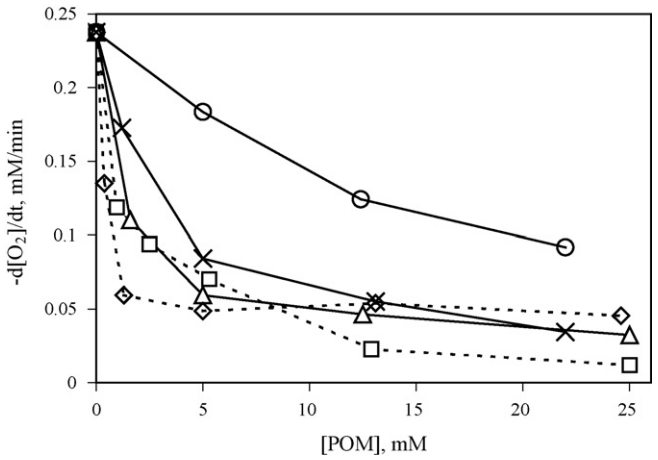

Fig. 5. Initial rates for oxidations of EtOH (0.82 M) by pure O_2 (1 atm) catalyzed by Pt/C (1.45 mg/mL; in 0.1 M $HClO_4$ at 25 °C), in the presence of α-$AlW_{12}O_{40}^{5-}$ (◯), α-$SiW_{12}O_{40}^{5-}$ (×), α-$PW_{12}O_{40}^{3-}$ (◊), α-$PMo_{12}O_{40}^{3-}$ (**1**; △), and $PV_2Mo_{10}O_{40}^{5-}$ (**2**; □).

and α-$PW_{12}O_{40}^{3-}$). The inhibition may thus be a consequence of one or more well documented correlations between POM reduction potential and chemical or physicochemical behavior. Namely, the POMs with more positive reduction potentials: (1) more rapidly oxidize radicals or other intermediates that may be present in solution or on the catalyst surface [20], (2) are more effective at oxidizing the surface of Pt(0) [21], and (3) are more favorably adsorbed on the Pt-surface [22]. While it must be stressed that the reactions and mechanistic steps involved are complex, and the Pt/C material itself poorly defined, the observed correlation between reduction potential and inhibition points to a common mechanism whereby POMs may act to inhibit the Pt/C catalyzed oxidation of alcohols. This observation is noteworthy in the more general context of ongoing efforts to understand and develop new chemical systems based on interactions between POMs and metal nanoparticles.

4. Conclusions

Data provided here demonstrate that two representative heteropolyanions, α-$PMo_{12}O_{40}^{3-}$ (**1**) and $PV_2Mo_{10}O_{40}^{5-}$ (**2**), are effective at "capturing" electrons during the Pt(0)-catalyzed *anaerobic* oxidation of alcohols at ambient temperature in water. No H_2 is observed. In addition, kinetic data show the reaction is independent of POM-anion concentration, such that, efficiency of electron transfer from glycerol (a model alcohol) to the POM "electron carriers" is limited by the effectiveness of the alcohol-oxidation catalyst. Potentiometric data indicate that the Pt(0)-catalyzed oxidations of the alcohols result in the two-electron reduction of **1**, and in substantial reduction of **2**. Upon exposure to O_2 in the presence of Pt/C, the reduced anions are rapidly oxidized to their (nearly) fully oxidized forms. Notably, this also applies to $\mathbf{1}_{1e}$, whose reactions with O_2 are typically very slow.

Finally, the data from this exploratory study are pertinent to the possible use of Keggin heteropolymolybdates as multi-functional (catalytic and electron-carrying) electrolytes in renewable-energy (biomass-based) fuel cells. More generally, the quantitative information provided here raises broader questions regarding whether POMs may in some instances enhance, or as in the present case, inhibit, reactions catalyzed by zero-valent late-transition metals or metal nanoparticles.

Acknowledgments

We thank the U.S. Department of Agriculture (FS-FPL-05-JV-11111122-026) for financial support. We also thank Robert Apkarian (The Integrated Microscopy and Microanalytical Facility, Emory University) for HREM data, and Craig L. Hill (Emory University) and Alan Rudie (USDA Forest Service, Forest Products Laboratory) for technical input and administrative support.

References

[1] M.Z. Jacobson, W.G. Colella, D.M. Golden, Science 308 (2005) 1901.
[2] Ford Unveils Hydrogen-Powered Shuttle Bus, Ford Motor Company, Detroit, MI, September 29, 2004, press release.
[3] National Hydrogen Energy Roadmap, U.S. Department of Energy, Washington, D.C., November 2002; U.S. DOE, Hydrogen Program, URL: http://www.hydrogen.energy.gov/.
[4] U.S. DOE, Office of Energy Efficiency and Renewable Energy (EERE) website, URL: http://www.eere.energy.gov/hydrogenandfuelcells/fuelcells/current_technology.html, November, 2004.
[5] B.C.L. Steele, A. Heinzel, Nature 414 (345) (2001).
[6] R.D. Cortright, R.R. Davda, J.A. Dumesic, Nature 418 (2002) 964.
[7] E. Chornet, S. Czernik, Nature 418 (2002) 928.
[8] A. Wieckowski, E.R. Savinova, C.G. Vayenas (Eds.), Catalysis and Electrocatalysis at Nanoparticle Surfaces, Marcel Dekker, New York, 2003.
[9] F. de Bruijn, Green Chem. 7 (2005) 132;
H.A. Gasteiger, S.S. Kocha, B. Sompalli, F.T. Wagner, Appl. Catal. B: Environ. 56 (2005) 9.
[10] J.R. Darwent, J. Chem. Soc., Chem. Commun. (1982) 709;
E.N. Savinov, S.S. Saidkhanov, V.N. Parmon, K.I. Zamaraev, Dokl. Phys. Chem. SSSR 272 (1983) 741;
T. Yamase, N. Takabayashi, M. Kaji, J. Chem. Soc., Dalton Trans. (1984) 793;
E. Papaconstantinou, Chem. Soc. Rev. 18 (1989) 1.
[11] C.L. Hill, D.A. Bouchard, J. Am. Chem. Soc. 107 (1985) 5148;
R.F. Renneke, C.L. Hill, J. Am. Chem. Soc. 110 (1988) 5461;
R.F. Renneke, M. Pasquali, C.L. Hill, J. Am. Chem. Soc. 112 (1990) 6585.
[12] I.M. Mbomekallé, F. Bian, H. Tebba, A. Müller, I.A. Weinstock, J. Cluster Sci., available on-line, May 25, 2006.
[13] A. Teze, G. Herve, Inorg. Synth. 27 (1990) 85;
I.A. Weinstock, J.J. Cowan, E.M.G. Barbuzzi, H. Zeng, C.L. Hill, J. Am. Chem. Soc. 121 (1999) 4608;
G.A. Tsigdinos, C.J. Hallada, Inorg. Chem. 7 (1968) 437.
[14] A. Selling, I. Andersson, J.H. Grate, L. Pettersson, Eur. J. Inorg. Chem. (2000) 1509.
[15] Yu.V. Geletii, C.L. Hill, A.J. Bailey, K.I. Hardcastle, R.H. Atalla, I.A. Weinstock, Inorg. Chem. 44 (2005) 8955;
Yu.V. Geletii, I.A. Weinstock, J. Mol. Catal. A: Chem. 251 (2006) 255.
[16] M.H. Barary, F.A. El-Yazbi, M.A. Bedair, Anal. Lett. 24 (1991) 857.
[17] I. Bar-Nahum, A.M. Khenkin, R. Neumann, J. Am. Chem. Soc. 126 (2004) 10236.

[18] W.B. Kim, T. Voitl, G.J. Rodriguez-Riveera, J.A. Dumesic, Nature 305 (2004) 1280;
I.A. Weinstock, E.M.G. Barbuzzi, M.W. Wemple, J.J. Cowan, R.S. Reiner, D.M. Sonnen, R.A. Heintz, J.S. Bond, C.L. Hill, Nature 414 (2001) 191.
[19] G.A. Camara, T. Iwasita, J. Electroanal. Chem. 578 (2005) 315.
[20] I.A. Weinstock, Chem. Rev. 98 (1998) 113.
[21] T. Mallat, A. Baiker, Appl. Catal. A 86 (1992) 147.
[22] E.D. Mishina, G.A. Tsirlina, E.V. Timofeeva, N.E. Sherstyuk, M.I. Borzenko, N. Tanimura, S. Nakabayashi, O.A. Petrii, J. Phys. Chem. B 108 (2004) 17096.